

# Hydration Reaction of Cementitious Materials Prepared with Molybdenum Tailings

Yanqing Di<sup>a,b</sup>, Xiaowei Cui<sup>a,b\*</sup>, Ning Nan<sup>a,b</sup>, Chunsheng Zhou<sup>a,b</sup>

<sup>a</sup> College of Chemical Engineering and Modern Materials, Shangluo University, Shangluo 726000, China;

<sup>b</sup> Shaanxi Key Laboratory of Comprehensive Utilization of Tailings Resources, Shangluo 726000, China  
 cuixiaowei8899@163.com

Cementitious materials is prepared with blended powders including molybdenum tailings, slag, clinker and gypsum. The effect of molybdenum tailings proportion on strengths and hydration products of molybdenum-tailing-based neat paste are studied. The results indicate that the compressive strength of neat paste decreases gradually with the increase of molybdenum tailings proportion. The relatively appropriate molybdenum tailings proportion in cementitious materials is 30%. The compressive strength of molybdenum-tailing-based neat paste is high up to 43.10 MPa cured at 28 days. The ground molybdenum tailings have a certain reactivity in the studied system. The hydration products of cementitious materials prepared with molybdenum tailings are mainly ettringite (AFt) and C-S-H gel.

## 1. Introduction

As the new century begins, mineral resources have played an increasingly important role in the rapidly developing mining and metallurgical economy (Yu, 2015; Bi and Dong, 2014). With the continuous exploitation of mineral resources, the ensuing environmental problems have become a global concern that is discussed and addressed concertedly. Shangluo City is an important producing area of molybdenum with abundant molybdenum ore resources, generating a large number of molybdenum tailings in the process of molybdenum ore tailings development and utilization, which locate in the source of Danjiang River. As the city is the water conservation area of the central line project of south-north water transfer. It is of particular significance as to how to make efficient use of molybdenum tailings. In the comprehensive utilization of molybdenum tailings, Di et al., (2016) prepared high-performance molybdenum tailings insulation materials and concrete materials used for external walls. Guo et al., (2011) made premium cement clinker from molybdenum tailings. However, there are little studies conducted on the hydration reaction mechanism of molybdenum tailings cementitious materials. Therefore, it is necessary to systematically study the hydration reaction mechanism of molybdenum tailings cementitious materials, which can lay a theoretical foundation for the comprehensive utilization of molybdenum tailings. In this study cementitious materials were prepared with solid wastes such as molybdenum tailings, slag and desulfurized gypsum, which has not been reported. Then, the influence of molybdenum tailings proportion on the hydration reaction mechanism was discussed.

## 2. Test materials and research methods

### 2.1 Test materials

Molybdenum tailings: taken from the underlying tailings pond of Kowloon Mining Co., Ltd., Luonan County, Shaanxi Province, at the bulk density of  $2.49\text{g}\cdot\text{m}^{-3}$ . As in Figure 1, the XRD pattern of the molybdenum tailings indicate that the major minerals of the molybdenum tailings are quartz, feldspar, phlogopite, and a small amount of amphibole and pyrite. Slag: blast furnace water quenching slag provided by the Hebei Jintai Cheng Building Materials Co., Ltd., at the bulk density of  $2.89\text{g}/\text{cm}^3$ . We also use the common Portland cement clinker and desulphurized gypsum produced by Shangluo Yaobo Longqiao Cement Company. Water: tap water. The main chemical composition of the main raw materials is shown in Table 1.

## 2.2 Test methods

The molybdenum tailings, slag and clinker were dried at 100 °C in an electric thermostatic dry blast box (DHG-9420A), and the gypsum was dried at 60 °C. After all the raw materials were dried, the moisture content was lower than 1 %. The specific surface areas of each powder ground by the cement test ball mill were 580 m<sup>2</sup>·kg<sup>-1</sup>, 560 m<sup>2</sup>·kg<sup>-1</sup>, 560 m<sup>2</sup>·kg<sup>-1</sup>, and 540 m<sup>2</sup>·kg<sup>-1</sup>, respectively. The ground material was mixed according to the scheme shown in Table 2 at the water-cement ratio of 0.20, and a 30 mm×30 mm×50 mm slurry was prepared. The standard cement curing box (YH-40B) was used to cure the paste sample. The influence of molybdenum tailings proportion on the compressive strength of cementitious materials was studied at the predetermined age according to GB /T 50081-2002 "Standard Test Method for Normal Concrete Mechanical Properties". And the hydration products of cementitious materials were studied by using XRD, DTA-TG IRand SEM-EDS.

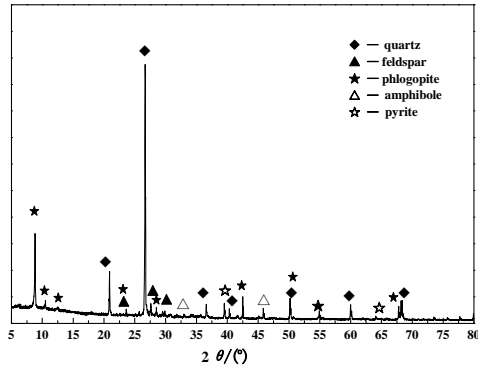


Figure 1: XRD patterns of molybdenum tailings

Table 1: The main chemical composition of the test raw materials (mass fraction, %)

Material	SiO <sub>2</sub>	Al <sub>2</sub> O <sub>3</sub>	TFe	MgO	CaO	Na <sub>2</sub> O	K <sub>2</sub> O	TiO <sub>2</sub>	P <sub>2</sub> O <sub>5</sub>	MnO	SO <sub>3</sub>	LOSS
molybdenum tailings	72.23	3.89	9.27	1.08	2.25	0.27	1.93	1.06	0.13	0.22	5.00	2.56
Slag	34.75	14.69	0.70	10.52	35.37	0.29	0.35	0.98		0.68	1.11	--
Clinker	22.37	3.46	3.47	0.83	65.30	--	1.47	0.81	--	--	0.31	0.96
Gypsum	3.20	1.37	0.59	7.36	33.58	0.13	0.18	--	0.13	--	45.75	7.28

Table 2: Preparation of molybdenum tailings cementitious materials/ %

Sample No.	Molybdenum tailings	Slag	Clinker	Gypsum
1	10	70	10	10
2	20	60	10	10
3	30	50	10	10
4	40	40	10	10

## 3. Test results and analysis

### 3.1 The effect of molybdenum tailings content on the mechanical properties of the slurry

The compressive strength of the paste sample was tested at 3d, 7d and 28d, respectively. The effect of the molybdenum tailings content on the compressive strength of the mortar block is shown in Fig. 2.

It can be seen from Fig. 2 that with the prolongation of reaction time, the compressive strength of the paste sample increases gradually, indicating that the hydration reaction is carried out continuously. At the same age, with the increases of molybdenum tailings proportion in cementitious materials, the compressive strength of the paste sample decreases gradually. When molybdenum tailings proportion increases from 10% to 20%, the compressive strength of the paste sample decreases by 13.96%, 9.05% and 4.06% at 3d, 7d and 28d, respectively. When molybdenum tailings proportion was lifted from 20% to 30%, the compressive strength decreased by 19.77%, 10.60% and 7.87%, respectively. When molybdenum tailings proportion increases from 30% to 40%, the compressive strength of the paste sample decreases by 44.2%, 29.64% and 24.59%, respectively, at 3d, 7d and 28d. Obviously, when molybdenum tailings proportion increases from 10% to 30%, the compressive strength of the paste sample will decrease more or less; while when molybdenum tailings

proportion increases from 30% to 40%, the decrease of the compressive strength is much more obviously, which is mainly due to the fact that molybdenum tailings are low-active. The gradual increment of molybdenum tailings results in the decrease of low-active composites and the reduction in hydration products produced thereby. Considering the compressive strength of the paste sample and the utilization rate of molybdenum tailings, it is more appropriate to determine molybdenum tailings proportion as 30%.

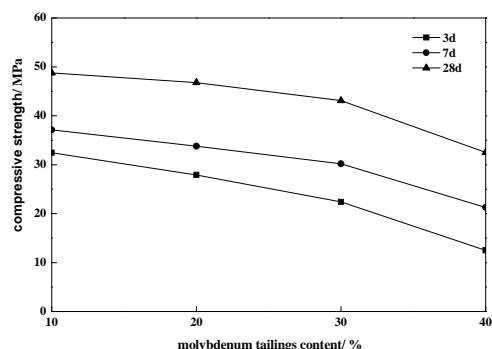


Figure 2: Effect of molybdenum tailings content on compressive strength of the paste sample

### 3.2 XRD Analysis of Paste Samples

The XRD pattern of the cementitious materials paste sample with 30% molybdenum tailings is shown in Figure 3.

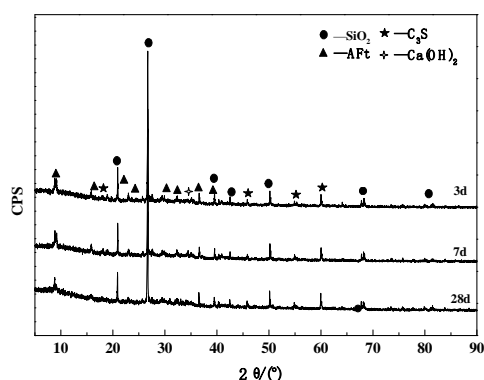


Figure 3: XRD patterns of the paste sample of molybdenum tailings cementitious materials

It can be seen from Figure 3 that the major phase of the hydration products of molybdenum tailings cementitious materials are quartz, calcium hydroxide, ettringite, and tricalcium silicate. The diffraction peak that falls in the range of  $25^{\circ}$  to  $35^{\circ}$  has a background of "convex hull", which is mainly the C-S-H gel produced by the hydration reaction (Wu et al., 2014). The diffraction peak of AFt is also increasing with the prolongation of the reaction time, indicating that the hydration reaction of the cementitious materials is proceeding continuously. The diffraction peaks of C-S-H and AFt have been found at the age of 3d. The diffraction peaks of quartz in the XRD pattern are mainly due to the fact that the molybdenum tailings are contained in cementitious materials. But its diffraction peak decreases slightly over time, indicating that some molybdenum tailings particles participate in the hydration reaction (Cui, Di and Nan, 2017). At the age of 28d, the diffraction peak of phlogopite is no longer obvious, indicating that it has participated in hydration reaction (Zhang, 2012). In addition, pyrite will gradually dissolve under the excitation of gypsum, for which iron ions will be converted into ferric hydroxide gel. This production can be intertwined with AFt and C-S-H gel as a whole to strengthen the system (Zheng, 2009). With the continuous progress of the hydration reaction, desulphurized gypsum excites the dissociation between slag and clinker and the re-bonding with molybdenum tailings particles. As a result, the amount of hydration products gradually increase, and the strength of the test piece is strengthened.

### 3.3 DTA-TG analysis

Figure 4 shows the DTA-TG curve of the cementitious materials after hydrated for 28 days.

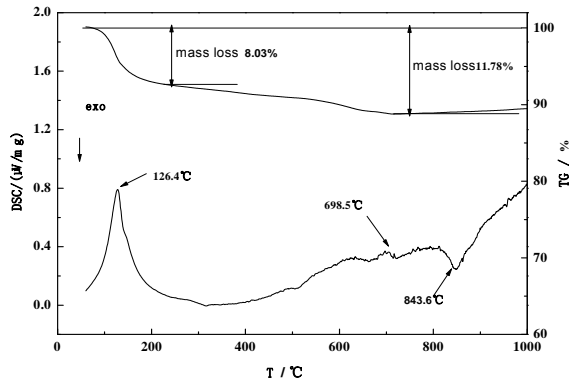


Figure 4: DTA-TG curve of cemented material hydrated for 28 days

It can be seen from Fig. 4 that there are two common endothermic peaks and one exothermic valley in the temperature range below 1000 °C on the DTA-TG curve of the paste sample: the endothermic peak at 126 °C is a dehydrated endothermic peak of AFt and the C-S-H gel. The endothermic peak at 698 °C is caused by the non-hydration of  $\beta$ -C<sub>2</sub>S to  $\alpha$ -C<sub>2</sub>S in the clinker. The exothermic valley around 840 °C reflects the production of Wollastonite from C-S-H gel (El- Didamony et al. 2013). From the DTA-TG diagram of the different hydration reaction time of the cementitious materials, the mass loss of the cementitious materials is 8.03% at the temperature of 30~200 °C, which is mainly due to the dehydration of the C-S-H gel and AFt, indicating that a large number of C-S-H gel and AFt are generated at the age of 28d, which is consistent with the conclusions in Figures 3.

### 3.4 FT-IR analysis

Figure 5 shows the FT-IR spectra of the molybdenum tailings cementitious materials clinkers at 3d, 7d and 28d.

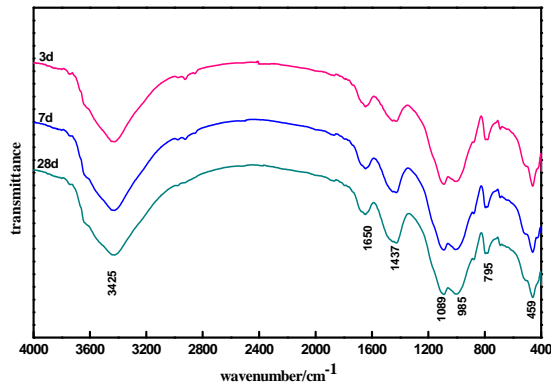


Figure 5: FT-IR spectrum of paste samples of molybdenum tailings cementitious materials

It is noticeable that all absorption peaks move towards small wave numbers in Fig. 4. In this figure, the Si-O bond's bending vibration occurs at 459 cm<sup>-1</sup>, the quartz's vibration absorption peak occurs at 795 cm<sup>-1</sup>, and the absorption peak at 985 cm<sup>-1</sup> is caused by the asymmetric vibration of Si-O in the silicon tetrahedral structure, which is also the characteristic peak of C-S-H gel (Yu, Kirkpatrick and POE, 1999, Huang et al. ,2013). The strong absorption band at 1089 cm<sup>-1</sup> is an asymmetric stretching vibration of the S-O bond (Wu, et al., 2014, Criado, Femandez-jimenez and Palomo, 2007), whose vibration peak gradually increases with the extension of the reaction time, indicating that AFt is successively formed, which is consistent with the results in Fig. 3. The absorption peaks at 985cm<sup>-1</sup> and 1089cm<sup>-1</sup> reflect the continuous generation of AFt and C-S-H gel. The absorption band at 1437cm<sup>-1</sup> is an asymmetric stretching vibration band of CO<sub>3</sub><sup>2-</sup> is possibly a result of the

carbonization of samples exposed to CO<sub>2</sub> in the air. The absorption band at 1650 cm<sup>-1</sup> is the bending vibration of the O-H bond in the water. The band at 3425 cm<sup>-1</sup> is the stretching vibration band of the bound water in the C-S-H gel, indicating that the C-S-H gel formation is successively generated over time. This is also consistent with the results of the analysis in Figure 3 and Figure 4.

### 3.5 SEM analysis

Figure 6 is the SEM images and EDS energy spectrum of cementitious materials hydrated at different ages.

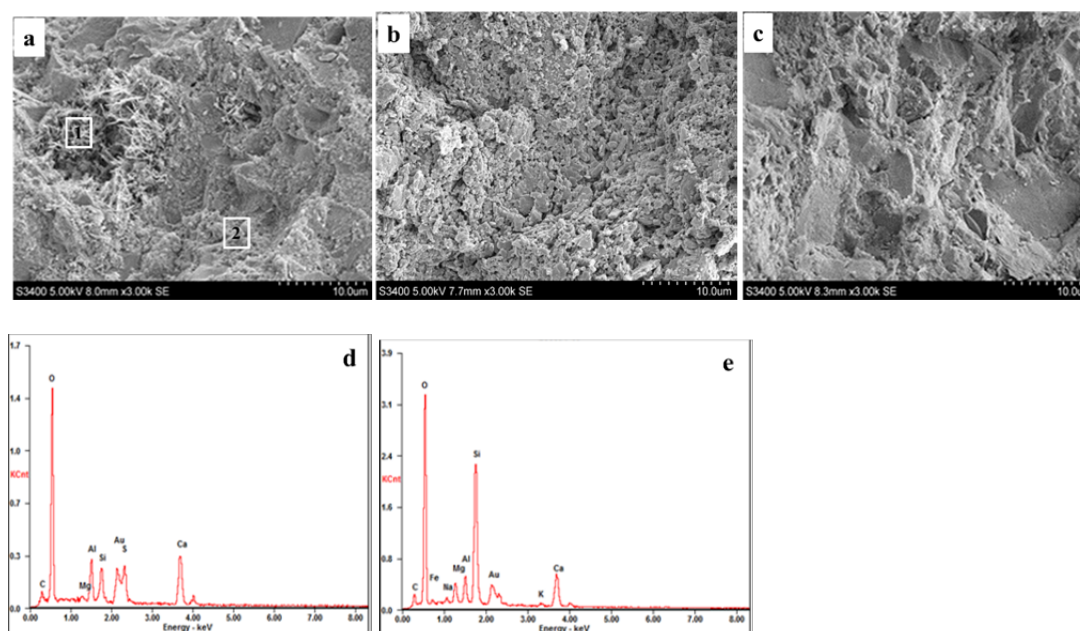


Figure 6: SEM images of cementitious materials hydrated at different ages (A: 3d; b: 7d; c: 28d; d: energy spectrum of point 1 in graph a; e: energy spectrum of point 2 in graph a)

It can be seen from Fig. 6 (a) that a large amount of hydrated product has been produced at the age of 3d. In light that the energy spectrum of point 1 includes elements of Ca, S, Al, Si and O, it should be AFt that are generated in this locality, in light that the energy spectrum of point 2 includes elements of Ca, Si and Al, it should be C-S-H gel that are produced in this point (Huang et al., 2016, Torres et al., 2008). These results proves the production of C-S-H gel and AFt at the age of 3d which enables the test piece to have a certain strength at an early age (Cui and Ni, 2016, Cui, Ni And Ren, 2016). In combination with Fig. 6 (b) and Fig. 6 (c), it is found that the number of hydrated products increases significantly with the increase of the curing age, and the C-S-H gel and ferric hydroxide gel has completely encompassed complete AFt at 28d. Their combination contributes to the dense internal structure of the cementitious materials sample and promotes the strength of the growth of the paste sample.

## 4. Conclusions

- (1) With the increase of molybdenum tailings proportion in cementitious materials, the compressive strength of paste decreases gradually, and the decrement is suddenly significant at the proportion of 40%. Therefore, the amount of molybdenum tailings in cementitious materials should not exceed 30%.
- (2) The hydration products of molybdenum tailings cementitious materials are AFt and C-S-H gel. With the increase of reaction age, the hydration products gradually increased. Also, the C-S-H gel and AFt and a small amount of ferric hydroxide gel that interweave with each other reduce the internal porosity of the test pieces and strengthens them.

## Acknowledgment

Authors would like to acknowledge the support by natural science foundation of Shaanxi province of China (2017JM5125), Comprehensive Utilization of Tailing Resources Key Laboratory of Shaanxi Province of China (2017SKY-WK003) and science and technology plan projects of Shangluo city of China (2014-01-03).

## References

- Bi X.W., Dong S.H., 2014, Progress and Prospect on High Efficient and Clean Utilization of Mineral Resources in China, *Bulletin of Mineralogy, Petrology and Geochemistry*, 33(1), 14-22.
- Criado M., Fernandez-jimenez A., Palomo A., 2007, Alkali activation of fly ash: effect of the  $\text{SiO}_2/\text{Na}_2\text{O}$  ratio Part I: FTIR study, *Microporous and Mesoporous Materials*, 106(1), 180-182.
- Cui X. W., Di Y. Q., Nan N., 2017, Grinding Characteristics of Vanadium Extracted Tailings from Stone Coal, *Journal of Shangluo University*, 31(2), 29-32, 60.
- Di Y.Q., Cui X.W., 2015, Preparation of High Performance Concrete with Iron Ore Tailings, *Journal of Shangluo University*, 6, 32-36.
- El-Didamony H., Amer A.A., El-Sokkary T.M., Abd-El-Aziz H., 2013, Effect of substitution of granulated slag by air-cooled slag on the properties of alkali activated slag, *Ceramics International*, 39(1), 171.
- Guo X.J., Yang Y.F., Lin H.Y., 2011, Research on the preparation of road cement clinker with molybdenum slag, *New Building Materials*, 5, 21-34.
- Huang X.L., Zhou S.B., Liang X.Y., Ren T.T., He F., 2013, FT-IR analysis of polymerization degree of different origin slag, *Sichuan Building Science*, 3, 226-229.
- Huang X., Wang Z., Liu Y., Hu W., Ni W., 2016, On the use of blast furnace slag and steel slag in the preparation of green artificial reef concrete, *Constr Build Mater*, 112, 241-246.
- Torres S.M., Kirk C.A., Lynsdale C. J., 2008, Thauasite--ettringite solid solutions in degraded mortars, *Cement Concrete Res*, 34(8), 1297-305.
- Wu H., Ni W., Cui X.W., Wang S., 2014, Preparation of concrete sleeper using hot steaming steel slag with low autogenous shrinkage, *Transactions of Materials and Heat Treatment*, 4, 7-12.
- Yu C.J., Li H.Q., Jia X.P., 2015, Improving resource utilization efficiency in China's mineral resource-based cities: A case study of Chengde, Hebei province, *Resources, Conservation and Recycling*, 94, 1-10.
- Yu P., Kirkpatrick R.J., POE B., Cong Y., 1999, Structure of calcium silicate hydrate (C-S-H): near-, mid-, and far-infrared spectroscopy, *J. Am. Ceram. Soc*, 82(3), 742-748.
- Zhang F.W., Yang J.T., Liu W.X., 2012, Microscopic experiment of consolidating tailings by slag cementing materials, *Journal of University of Science and Technology Beijing*, 34(7), 738-743.
- Zheng Y.C., Ni W., Zhang F., Wang H.X., Yang J.H., 2009, Test Research on Preparation of Fine Aggregate Concrete with Fine Iron Tailings, *Metal Mine*, 12, 151-153.